IEEE Photonics Journal
An IEEE Photonics Society Publication

Open Access

Dispersion Retrieval for Spatial-Spectral Interference of Ultra-Short Pulses

Volume 11, Number 6, December 2019

Jie Mu
Xiao Wang
Yanlei Zuo
Kainan Zhou
Bilong Hu
Xiaoming Zeng
Xiaodong Wang
Dongbin Jiang
Na Xie
Xiaojun Huang
Jingqin Su

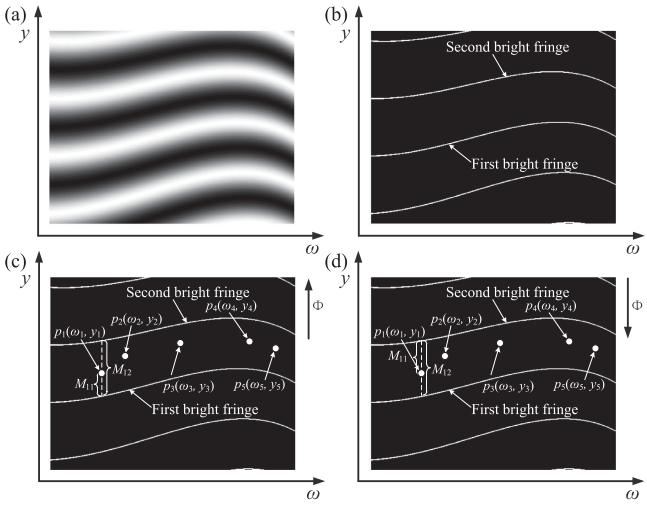

DOI: 10.1109/JPHOT.2019.2947363

IEEE photonics SOCIETY

IEEE

Dispersion Retrieval for Spatial-Spectral Interference of Ultra-Short Pulses

Jie Mu,[1,2,3] **Xiao Wang**,[1,2,3] **Yanlei Zuo**,[1,2,3] **Kainan Zhou**,[1,2,3] **Bilong Hu**,[1,2,3] **Xiaoming Zeng**,[1,2,3] **Xiaodong Wang**,[1,2,3] **Dongbin Jiang**,[1,2,3] **Na Xie**,[1,2,3] **Xiaojun Huang**,[1,2,3] **and Jingqin Su**[1,2,3]

[1]Laser Fusion Research Center, China Academy of Engineering Physics, Mianyang, Sichuan 621900, China
[2]Science and Technology on Plasma Physics Laboratory, Mianyang, Sichuan 621900, China
[3]Collaborative Innovation Center of IFSA, Shanghai Jiao Tong University, Shanghai 200240, China

DOI:10.1109/JPHOT.2019.2947363

Manuscript received July 21, 2019; revised September 29, 2019; accepted October 8, 2019. Date of publication October 14, 2019; date of current version November 11, 2019. This work was supported in part by the National Natural Science Foundation of China under Grant 61505188 and in part by the Science and Technology on Plasma Physics Laboratory under Grant 6142A04180303. Corresponding authors: Xiao Wang; Yanlei Zuo (e-mail: wangxiaocn@263.net; zuoyanlei@tsinghua.org.cn).

Abstract: Spatial-spectral interference is an effective way to characterize an unknown ultra-short pulse. The key of characterizing an unknown ultra-short pulse is to retrieve the dispersion. Considering that the spatial-spectral interference fringe is the equiphase line of different spectra in the space domain and that the phase difference between adjacent interferences is equal to 2π, we propose a novel method of dispersion retrieval for spatial-spectral interference. The analytic expression is deduced and demonstrated by simulated experiments. This method has the advantages of intuitive principle, less calculation and simple process with no Fourier transform, which are beneficial for practical applications.

Index Terms: Dispersion retrieval, spatial-spectral interference, short pulse.

1. Introduction

Ultra-short and -intense pulses can produce extreme states of matter in the laboratory and therefore open a path to many research fields, such as fast ignition [1], laser wake-field acceleration [2], and astrophysics in laboratory [3]. In the past few years, many ultra-short laser facilities have been developed or are under construction all over the world, e.g., the multi-PW laser facility named CAEP-PW in China [4], the 4.2 PW laser facility in Korea [5], Apollon 10 in France [6], Vulcan 10 PW in UK [7], ELI-Beams in Czech Republic [8] and the Russian Exawatt Center for Extreme Light Studies (XCELS) project [9].

To generate ultra-intense pulses, the techniques of Chirped pulse amplification (CPA) [10] and Optical Parametric Chirped Pulse Amplification (OPCPA) [11] are usually utilized in ultra-short laser facilities. During the stretching-amplification-compression process in CPA and OPCPA, a femtosecond (fs) pulse seeded by a mode-locked laser oscillator can be amplified to the petawatt (PW) peak power level. To achieve extremely high intensity, it is necessary to generate the ultra-short pulse with a near-Fourier-transform-limited duration. Several techniques are capable of characterizing ultra-short pulses, e.g., Spectral Phase Interferometry for Direct Electric-Field Reconstruction (SPIDER)

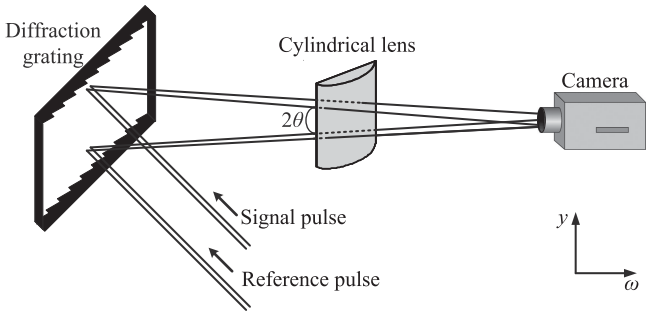

Fig. 1. Schematic of SSI.

[12], Frequency-Resolved Optical Gating (FROG) [13], and Spectral Interference (SI). SPIDER requires a complex apparatus and a pulse shape-dependent delay calibration, while FROG requires that a large amount of data be processed by an iterative algorithm. Therefore, both techniques are usually applied to simple pulse measurement. Furthermore, both SPIDER and FROG involve a nonlinear process, which limits their application to ultra-weak pulses. SI, a linear technique, can be used to measure the spectral phase difference between two pulses as weak as 42 zeptojoules [14].

As an improved version of SI, Spatial-Spectral Interference (SSI) [15] involves the spectral interference between two pulses crossing at a small angle. By integrating the interference in the spectral and spatial domains, SSI is easy to implement in practice. Moreover, SSI has the advantages of no sign ambiguity, no unwrapping operation, and high spectral resolution. Existing studies demonstrate that SSI is very useful for the dispersion control of a pulse compressor [16], the complex pulse characterization [17], the pulse shaper optimization [18], and other applications. A. P. Kovács *et al.* [19] and our research group [20] show that the group delay (i.e. time delay) between incident pulses can be determined by measuring the slope of SSI fringe. To acquire the spectral phase information in SSI, P. Bowlan *et al.* [21] propose Fourier-filtering the SSI trace in the spatial coordinate, and then isolating the spectral phase-containing term. Considering that the SSI fringe is the equiphase line of different spectra in the space domain and that the spectral phase difference between adjacent interferences is equal to 2π, we propose a novel dispersion retrieval method for SSI. Using this method, the dispersion of an incident pulse is directly extracted in the presence of high order dispersion with no Fourier transform processing required.

2. Theory

Fig. 1 shows the schematic of SSI. Two pulses, a signal pulse and a reference pulse, pass through a diffraction grating and a cylindrical lens with a crossing angle of 2θ. Then the optical frequencies of the two pulses are mapped at the focal plane of the cylindrical lens along the direction perpendicular to the grating grooves. The field along the parallel dimension, denoted as y, is not affected. The spatially and spectrally resolved interferogram is recorded by a camera placed at the focal plane of the cylindrical lens. The intensity I at a point (ω, y) can be described as

$$I(\omega, y) = I_{ref}(\omega) + I_{sig}(\omega) + 2\sqrt{I_{ref}(\omega)}\sqrt{I_{sig}(\omega)} \cdot \cos(2ky \sin\theta + \phi_{sig}(\omega) - \phi_{ref}(\omega)) \quad (1)$$

where ω is the angular frequency, k is the wave number, y is the spatial coordinate, $I_{ref}(\omega)$ and $I_{sig}(\omega)$ represent the spectral intensities of the reference and signal pulses, respectively, and $\phi_{ref}(\omega)$ and $\phi_{sig}(\omega)$ represent the spectral phases of the reference and signal pulses, respectively. When the reference and signal pulses are seeded by the same oscillator, their initial spectral phases are the same and are believed to be constant. Moreover, the reference pulse is usually a simple pulse with no dispersion. Consequently, the spectral phase difference between the two pulses can be

expanded into Taylor's series up to the third order around the central angular frequency ω_0 as

$$\phi_{sig}(\omega) - \phi_{ref}(\omega) = \omega t + \frac{\phi''}{2!}(\omega - \omega_0)^2 + \frac{\phi'''}{3!}(\omega - \omega_0)^3 \tag{2}$$

where t is the time delay between the two pulses, the primes denote the derivatives with respect to ω, and ϕ'' and ϕ''' are the group delay dispersion and the third order dispersion of the signal pulse, respectively. Let $\Phi(\omega, y) = 2ky\sin\theta + \phi_{sig}(\omega) - \phi_{ref}(\omega)$ represent the phase at the point (ω, y). Assuming that there are N points, $p_1, p_2, \ldots, p_N$, which are located in the same order interference region, it can be deduced that

$$\begin{pmatrix} \sin\theta \\ t \\ \phi'' \\ \phi''' \end{pmatrix} = \begin{pmatrix} \frac{2y(\omega_1-\omega_2)}{c} & \omega_1-\omega_2 & \frac{(\omega_1-\omega_0)^2-(\omega_2-\omega_0)^2}{2} & \frac{(\omega_1-\omega_0)^3-(\omega_2-\omega_0)^3}{6} \\ \frac{2y(\omega_1-\omega_3)}{c} & \omega_1-\omega_3 & \frac{(\omega_1-\omega_0)^2-(\omega_3-\omega_0)^2}{2} & \frac{(\omega_1-\omega_0)^3-(\omega_3-\omega_0)^3}{6} \\ \cdots & \cdots & \cdots & \cdots \\ \frac{2y(\omega_1-\omega_N)}{c} & \omega_1-\omega_N & \frac{(\omega_1-\omega_0)^2-(\omega_N-\omega_0)^2}{2} & \frac{(\omega_1-\omega_0)^3-(\omega_N-\omega_0)^3}{6} \end{pmatrix}^{-1} \begin{pmatrix} \Phi_1-\Phi_2 \\ \Phi_1-\Phi_3 \\ \cdots \\ \Phi_1-\Phi_N \end{pmatrix} \tag{3}$$

where the superscript of -1 represents the pseudoinverse of a matrix, c is the speed of light in vacuum, and $\omega_1, \ldots, \omega_N$ are the angular frequencies at the N points. From Eq. (3), we can acquire the parameters of θ, t, ϕ'', and ϕ'''. As a spatial carrier for the spectral information, the crossing angle between the two pulses determines the fringe spacing along the spatial direction. The time delay between the two pulses is determined by the optical path difference. ϕ'' and ϕ''' are the mainly characteristic parameters which determine the performance of the signal pulse.

With a value range of $[-1, 1]$, the cosine term in Eq. (1) causes a periodic change of the SSI intensity. The phase difference between adjacent order interference regions is equal to 2π, which means that the phases at the points between the two adjacent bright (or dark) fringes are $[0, 2\pi]$. Although the exact values of $\Phi_1, \Phi_2, \ldots,$ and Φ_N are uncertain because of the uncertain interference order, the values of $\Phi_1 - \Phi_2, \Phi_1 - \Phi_3, \cdots,$ and $\Phi_1 - \Phi_N$ can be estimated by an equal interval sampling of the interferogram in the space domain. Fig. 2 illustrates how to estimate the phase difference at different points. Fig. 2(a) is a simulated interferogram of SSI for two pulses. After a two-valued operation, a series of bright fringes are listed, as shown in Fig. 2(b). Two adjacent fringes are selected, denoted as the first bright fringe and the second bright fringe. Five points in the region between the two fringes are labeled as p_1, p_2, p_3, p_4, and p_5. Taking the phase of p_1 for example, $\Phi_1 = 2n\pi + 2\pi M_{11}/M_{12}$ (n is the order of interference and is an integer), where M_{12} is the spatial distance crossing the point between the two fringes. If Φ increases in the positive direction of y, M_{11} is the spatial distance between p_1 and the first bright fringe, while M_{11} is that between p_1 and the second bright fringe if Φ increases in the negative direction of y, as depicted in Fig. 2(c) and Fig. 2(d), respectively. The phases at the other points can also be acquired in this way. The five points are in the same interference order, which means that n is eliminated for the phase difference calculation. Hence, the exact value of n is not required.

Fig. 3 shows the flow chart of the dispersion retrieval for SSI. There are four steps to follow.

S1: Obtain the two-valued result of the SSI interferogram;

S2: Select two adjacent bright fringes and N points that are located in the region between the two bright fringes, and record the angular frequencies $\omega_1, \omega_2, \ldots, \omega_N$, and the spatial coordinates $y_1, y_2, \ldots, y_N$;

S3: Calculate the phase differences $\Phi_1 - \Phi_2, \Phi_1 - \Phi_3, \ldots,$ and $\Phi_1 - \Phi_N$ by an equal interval sampling of the interferogram in the space domain introduced in the above section;

S4: Substitute the phase differences, the angular frequencies, and the spatial coordinates into Eq. (3) and acquire the dispersion parameters of the signal pulse.

It should be noted that the change tendency of the phase (i.e., Φ) in the direction of the spatial domain (i.e., y) must be calibrated first. By analyzing the optical arrangement, specifically which pulse travels upward and which travels downward where the two pulses cross, the change tendency of the phase can be confirmed. It can also be tested by inserting a known standard film in the optical path. A minimum of five sampling points are required because there are four unknown terms θ, t, Φ'',

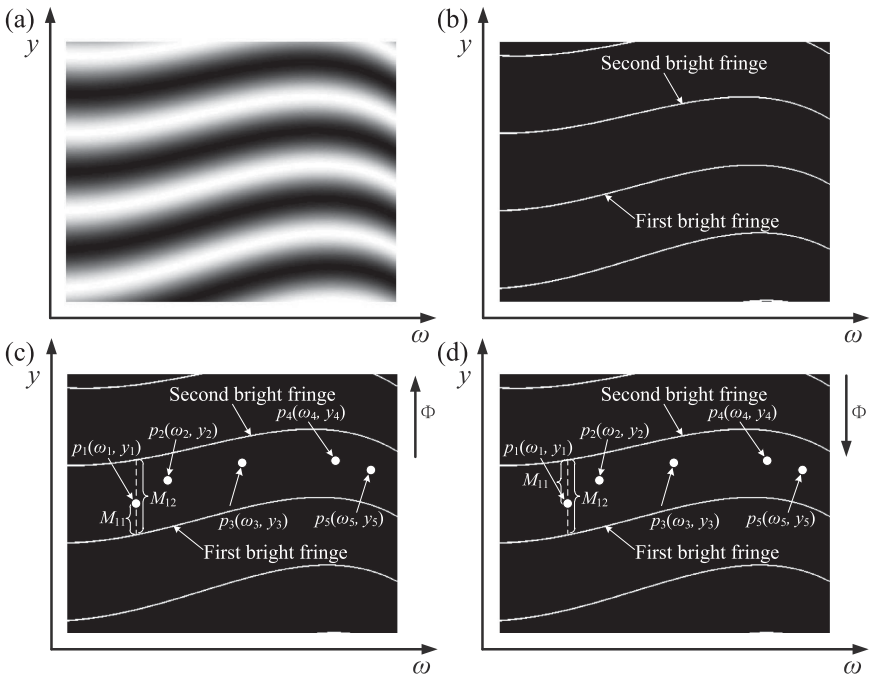

Fig. 2. Estimation of phase difference at different points: (a) simulated interferogram of SSI for two pulses; (b) two-valued result of (a); (c) phase estimation if the phase increases in the positive direction of y; (d) phase estimation if the phase increases in the negative direction of y.

and Φ'''. The more the sampling points, the higher the calculation accuracy. In Fig. 3, looping steps S2 to S3 can be performed to select multiple adjacent bright fringes for additional sampling points. Of course, the dark fringes can also be selected instead of the bright ones.

SSI carries the spectral phase difference information between the incident pulses. In the above derivation, a reference pulse with no dispersion is assumed. In this case, the extracted dispersion originates only from the signal pulse. When the dispersion of the reference pulse is nonzero, it should be measured beforehand. Because the reference pulse is usually a simple pulse originating from an oscillator, it can be easily measured by SPIDER or FROG.

3. Simulation

To test the suitability of the above-mentioned method, two simulated experiments are performed. The following two examples show the retrieval of the parameters of t, Φ'', and Φ'''. Fig. 2(a) shows the simulated SSI interferogram for the conditions $\theta = 0.02^\circ$, $\omega_0 = 2.3562e^{15}$ rad/s (corresponding to the central lambda of 800 nm), $t = -15$ fs, $\Phi'' = -88$ fs^2, and $\Phi''' = 1400$ fs^3. The phase increases in the positive direction of y. We use the five sampling points in Fig. 2(c) to calculate the parameters of t, Φ'', and Φ'''. As shown in Table 1, the angular frequencies of the sampling points are $2.35e^{15}$ rad/s, $2.3921e^{15}$ rad/s, $2.49e^{15}$ rad/s, $2.6136e^{15}$ rad/s, and $2.66e^{15}$ rad/s, respectively, and their spatial coordinates are $-1e^{-5}$ m, $3.5e^{-4}$ m, $6.2e^{-4}$ m, $6.5e^{-4}$ m, and $5.1e^{-4}$ m, respectively. The phase differences $\Delta\Phi$ of $\Phi_1 - \Phi_2$, $\Phi_1 - \Phi_3$, $\Phi_1 - \Phi_4$, and $\Phi_1 - \Phi_5$ are -1.345 rad, -1.3085 rad, -1.1202 rad, and -1.0648 rad, respectively. According to Eq. (3), the computed t, Φ'', and Φ''' are -16.2 fs, -85.9 fs^2, and 1437.6 fs^3, respectively.

Fig. 4(a) shows the simulated SSI interferogram for a set of different conditions: $t = 80$ fs, $\Phi'' = 200$ fs^2, $\Phi''' = -5000$ fs^3. The phase increases in the negative direction of y. We use the six sampling points shown in Fig. 4(b) to calculate the parameters of t, Φ'', and Φ'''. With reference to previous discussions, $\Phi_1 = 2n\pi + 2\pi M_{11}/M_{12}$ (M_{11}, and M_{12} are shown in Fig. 4(b)). The phases at the other

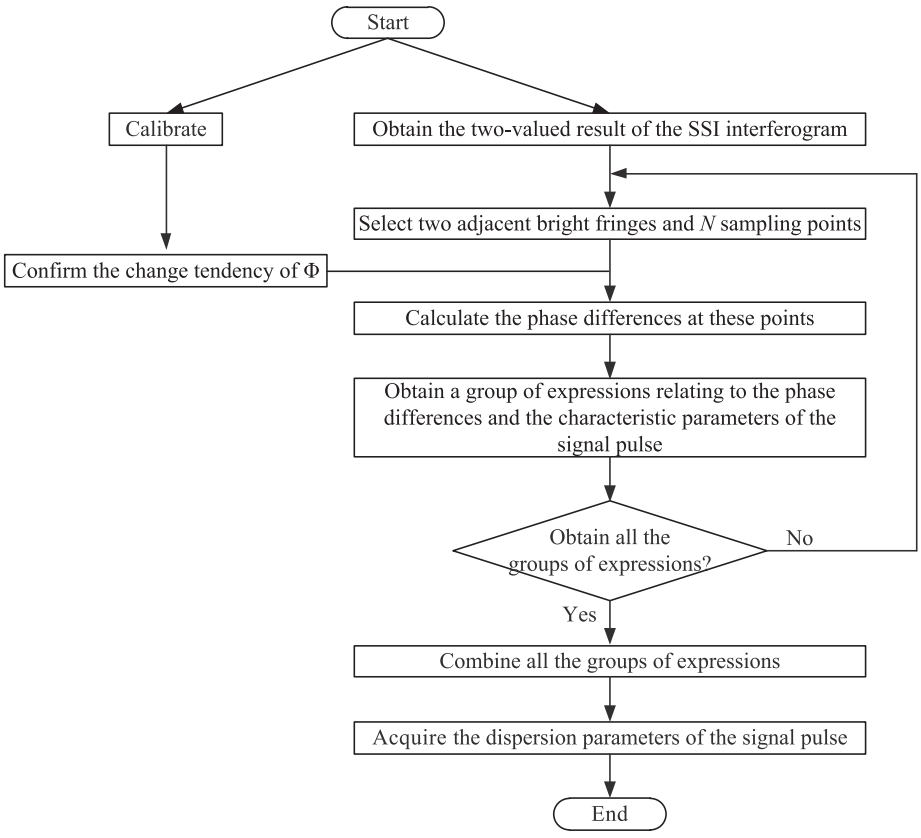

Fig. 3. Flow chart of the dispersion retrieval for SSI.

TABLE 1
Simulation Result of Fig. 2

	ω	y	$\Delta\Phi$	t	Φ''	Φ'''
	$e^{15}\ rad/s$	$e^{-4}\ m$	rad	fs	fs^2	fs^3
p_1	2.35	-0.1				
p_2	2.3921	3.5	-1.345			
p_3	2.49	6.2	-1.3085	-16.2	-85.9	1437.6
p_4	2.6136	6.5	-1.1202			
p_5	2.6601	5.1	-1.0648			

five points are similar to Φ_1. The angular frequencies of the sampling points are $2.3896e^{15}$ rad/s, $2.4576e^{15}$ rad/s, $2.5053e^{15}$ rad/s, $2.5814e^{15}$ rad/s, $2.6586e^{15}$ rad/s, and $2.6851e^{15}$ rad/s, respectively, and their spatial coordinates are $-1.4e^{-3}$ m, $-2e^{-4}$ m, $4e^{-4}$ m, $6e^{-4}$ m, $4e^{-4}$ m, and $-1e^{-4}$ m, respectively. The phase differences $\Delta\Phi$ of $\Phi_1 - \Phi_2$, $\Phi_1 - \Phi_3$, $\Phi_1 - \Phi_4$, $\Phi_1 - \Phi_5$, and $\Phi_1 - \Phi_6$ are 0.8111 rad, 1.1618 rad, 0.5955 rad, 2.7197 rad, and 2.0914 rad, respectively. As shown in Table 2, the computed t, Φ'' and Φ''' are 82.2 fs, 201.3 fs^2, and -5095.3 fs^3, respectively.

It can be seen that the simulation results of Fig. 2 and Fig. 4 closely match the settings, verifying the suitability of this proposed method for dispersion retrieval. Because of the limited spatial resolution, imperfect two-valued SSI interferogram, and finite sampling points, the simulation results are not exactly the same as the settings.

In practical applications, the SSI interferogram is usually affected by the inevitable noise, nonuniform near-field arrangement of the pulse, imperfect surface of the optics, and so on. In this

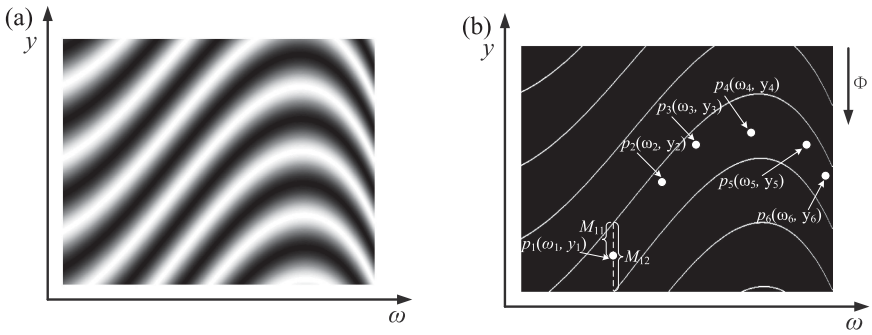

Fig. 4. Dispersion retrieval for SSI: (a) simulated interferogram of SSI for two pulses; (b) two-valued result of (a).

TABLE 2
Simulation Result of Fig. 4

	ω	y	$\Delta\Phi$	t	Φ''	Φ'''
	$e^{15}\ rad/s$	$e^{-4}\ m$	rad	fs	fs^2	fs^3
p_1	2.3896	-14				
p_2	2.4576	-2	0.8111			
p_3	2.5053	4	1.1618	82.2	201.3	-5095.3
p_4	2.5814	6	0.5955			
p_5	2.6586	4	2.7197			
p_6	2.6851	-1	2.0914			

condition, the local region of the SSI interferogram which is less affected should be selected to perform the calculation.

4. Conclusion

In this paper, we present a novel method of dispersion retrieval for SSI. The analytic expression is deduced based on the SSI fringe being the equiphase line of different spectra in the space domain. Two examples are simulated to demonstrate the suitability of this proposed method. With the advantages of intuitive principle, less calculation and simple process with no Fourier transform, this method is applicable to the dispersion measurement and control for achieving near Fourier-transform-limited ultra-short pulses, coherent combination of multiple ultra-short pulses, and other applications.

References

[1] R. Kodama *et al.*, "Fast heating of ultrahigh-density plasma as a step towards laser fusion ignition," *Nature*, vol. 412, pp. 798–802, 2001.
[2] A. E. Hussein *et al.*, "Laser-wakefield accelerators for high-resolution X-ray imaging of complex microstructures," *Sci. Rep.*, vol. 9, 2019, Art. no. 3249.
[3] S. Fujioka *et al.*, "X-ray astronomy in the laboratory with a miniature compact object produced by laser-driven implosion," *Nature Phys.*, vol. 5, pp. 821–825, 2009.
[4] X. M. Zeng *et al.*, "Multi-petawatt laser facility fully based on optical parametric chirped-pulse amplification," *Opt. Lett.*, vol. 42, pp. 2014–2017, 2017.
[5] J. H. Sung *et al.*, "4.2 PW, 20 fs Ti:sapphire laser at 0.1 Hz," *Opt. Lett.*, vol. 42, pp. 2058–2061, 2017.
[6] J. P. Zou *et al.*, "Design and current progress of the Apollon 10 PW project," *High Power Laser Sci. Eng.*, vol. 3, no. e2, pp. 1–4, 2015.
[7] C. H.-Gomez *et al.*, "The vulcan 10 PW project," *J. Phys.: Conf. Ser.*, vol. 244, 2010, Art. no. 032006.

[8] B. Le Garrec *et al.*, "ELI-Beamlines: Extreme light infrastructure science and technology with ultra-intense lasers," *Proc. SPIE*, vol. 8962, 2014, Art. no. 896201.
[9] A. V. Bashinov, A. A. Gonoskov, A. V. Kim, G. Mourou, and A. M. Sergeev, "New horizons for extreme light physics with mega-science project XCELS," *Eur. Phys. J. Special Topics*, vol. 223, pp. 1105–1112, 2014.
[10] D. Strickland and G. Mourou, "Compression of amplified chirped optical pulses," *Opt. Commun.*, vol. 56, pp. 219–221, 1985.
[11] A. Dubietis, G. Jonušauskas, and A. Piskarskas, "Powerful femtosecond pulse generation by chirped and stretched pulse parametric amplification in BBO crystal," *Opt. Commun.*, vol. 88, pp. 437–440, 1992.
[12] M. E. Anderson, A. Monmayrant, S.-P. Gorza, P. Wasylczyk, and I. A. Walmsley, "SPIDER: A decade of measuring ultrashort pulses," *Laser Phys. Lett.*, vol. 5, pp. 259–266, 2008.
[13] D. J. Kane and R. Trebino, "Characterization of arbitrary femtosecond pulses using frequency-resolved optical gating," *IEEE J. Quantum Electron.*, vol. 29, no. 2, pp. 571–579, Feb. 1993.
[14] D. N. Fittinghoff *et al.*, "Measurement of the intensity and phase of ultraweak, ultrashort laser pulses," *Opt. Lett.*, vol. 21, pp. 884–886, 1996.
[15] D. Meshulach, D. Yelin, and Y. Silberberg, "Real-time spatial-spectral interference measurements of ultrashort optical pulses," *J. Opt. Soc. Am. B*, vol. 14, pp. 2095–2098, 1997.
[16] Y. L. Zuo *et al.*, "Alignment of a petawatt-class pulse compressor with the third-order dispersion completely compensated," *Laser Phys. Lett.*, vol. 13, 2016, Art. no. 055302.
[17] P. Bowlan, P. Gabolde, M. A. Coughlan, R. Trebino, and R. J. Levis, "Measuring the spatiotemporal electric field of ultrashort pulses with high spatial and spectral resolution," *J. Opt. Soc. Amer. B*, vol. 25, pp. A81–A92, 2008.
[18] J. J. Field, T. A. Planchon, W. Amir, C. G. Durfee, and J. A. Squier, "Characterization of a high efficiency, ultrashort pulse shaper incorporating a reflective 4096-element spatial light modulator," *Opt. Commun.*, vol. 278, pp. 368–376, 2007.
[19] A. P. Kovács, K. Osvay, Zs. Bor, and R. Szipöcs, "Group-delay measurement on laser mirrors by spectrally resolved white-light interferometry," *Opt. Lett.*, vol. 20, pp. 788–790, 1995.
[20] J. Mu *et al.*, "Time delay retrieval via the slope of spatial-spectral interference fringe for short pulses," *Proc. SPIE*, vol. 11052, 2019, Art. no. 1105209.
[21] P. Bowlan, P. Gabolde, A. Shreenath, K. McGresham, and R. Trebino, "Crossed-beam spectral interferometry: A simple, high-spectral-resolution method for completely characterizing complex ultrashort pulses in real time," *Opt. Exp.*, vol. 14, pp. 11892–11900, 2006.